NATIONAL ADVISORY COMMITTEE FOR AERONAUTICS

TECHNICAL NOTE

No. 1093

EFFECT OF SWEEPBACK AND ASPECT RATIO ON LONGITUDINAL STABILITY CHARACTERISTICS OF WINGS AT LOW SPEEDS

By Joseph A. Shortal and Bernard Maggin

Langley Memorial Aeronautical Laboratory
Langley Field, Va.

Washington
July 1946

NATIONAL ADVISORY COMMITTEE FOR AERONAUTICS

TECHNICAL NOTE No. 1093

EFFECT OF SWEEPBACK AND ASPECT RATIO ON LONGITUDINAL STABILITY CHARACTERISTICS OF WINGS AT LOW SPEEDS

By Joseph A. Shortal and Bernard Maggin

SUMMARY

Because of the interest in swept-back wings for high-speed airplanes an analysis has been made of readily available data on the longitudinal stability characteristics of swept-back wings at low speeds. The analysis indicated that the shape of the pitching-moment curve near the stall for swept-back wings is greatly dependent upon the aspect ratio. A chart has been prepared relating aspect ratio and sweepback that indicates the combinations of aspect ratio and sweepback necessary to obtain stability near the stall for wings alone. The effect of the addition of a horizontal tail behind a swept-back wing may be destabilizing and requires further investigation.

INTRODUCTION

The use of swept-back wings and tail surfaces on airplanes has the distinct advantage of increasing the critical Mach number of the surfaces. High degrees of sweepback offer the possibility of flight at supersonic speeds without serious compressibility effects. On the other hand, sweepback has the disadvantage of introducing additional stability problems at low airspeeds, particularly at high angles of attack. One of these problems, which was encountered previously with tailless airplanes having swept-back wings at low speeds, is longitudinal instability at the stall. In an attempt to isolate the factors affecting this type of instability an analysis has been made of readily available data on swept-back wings for a range of sweepback angle from 0° to 80° and for wide ranges of aspect ratio and taper ratio. The basic longitudinal stability characteristics for the wings investigated are given in the present paper along with a chart summarizing the results of the investigations. In addition, some data are given for combinations of wings and horizontal tails to indicate the possible influence of the horizontal tail on the pitching moments. The effects of flaps are not considered and all the data were obtained at relatively low Reynolds numbers and Mach numbers.

SYMBOLS

C_L lift coefficient $\left(\frac{\text{Lift}}{qS}\right)$

C_D drag coefficient $\left(\frac{\text{Drag}}{qS}\right)$

C_m pitching-moment coefficient $\left(\frac{\text{Pitching moment}}{q\bar{c}S}\right)$; used with subscript to denote longitudinal reference axis as fraction of mean aerodynamic chord

q dynamic pressure, pounds per square foot $\left(\frac{1}{2}\rho V^2\right)$

ρ air density, slugs per cubic foot

V airspeed, feet per second

S wing area, square feet

b wing span, feet

$\bar{c}$ mean aerodynamic chord, feet

c_r root chord, feet

c_t tip chord, feet

t airfoil thickness, feet

A aspect ratio (b^2/S)

l_t distance between center of gravity and quarter chord of mean aerodynamic chord of horizontal tail, feet

h_t height of horizontal tail measured perpendicular to extended root chord of wing, feet

R test Reynolds number; no correction for turbulence factor

α angle of attack, degrees

Λ angle of sweepback of quarter-chord line, degrees

λ taper ratio $\left(\frac{\text{Tip chord}}{\text{Root chord}}\right)$

METHOD OF PRESENTATION OF DATA

The basic data on the longitudinal stability characteristics of wings with a range of sweepback angle from 0° to 80° and various taper ratios and aspect ratios are presented in figures 1 to 38. Figures 39 and 40 present data showing the effect of slats and wing twist on the longitudinal stability characteristics. On each figure the plan form of the model tested, the geometric and test parameters of interest, and the source of the data are given. The data are presented in the form of curves of C_L, C_D, and C_m against α and of C_L against C_m. In order to establish a basis for comparison of the various pitching-moment curves all the pitching-moment data have been transferred to a center-of-gravity location which results in a static margin of 5 percent mean aerodynamic chord $\left(\frac{-dC_m}{dC_L} = 0.05\right)$ at zero lift. The subscripts after C_m give the location of the center of gravity to which the moments have been transferred. The results of the analysis of these data are summarized in figure 41.

The results of tests of models with swept-back wings and horizontal tails are presented in figures 42 to 45. These data have also been referred to a center-of-gravity location resulting in a static margin of 5 percent mean aerodynamic chord at zero lift.

WINGS

The pitching-moment characteristics of a collection of swept-back wings and wing and fuselage combinations are examined first. The effect of sweepback in promoting stalling at the wing tips and in producing longitudinal instability near maximum lift is well known. Flow separation and loss of lift over parts of the wing behind the center of gravity usually result in a pronounced nose-up pitching moment. The longitudinal stability characteristics of a series of three wings of constant aspect ratio 6 but of varying sweepback from 0° to 30° presented in figures 1 to 3 show this effect quite clearly. The wing with 0° sweepback had a pronounced nose-down pitching moment at the stall. The wing with 15° sweepback had a similar change in pitching moment, whereas the wing with 30° sweepback became quite unstable at the stall. The results from tests of two other wings with approximately 30° sweepback but higher aspect ratios (7 and 11.9) presented in figures 4 and 5 indicated that an increase in aspect ratio increased the degree of instability. Even with only 15° sweepback instability was encountered with a wing of aspect ratio 12, as shown in figure 6. Reducing the aspect ratio of wings having 30° sweepback to 4.36 and to 3.0 resulted in stability, as shown in figures 8 and 9. With larger amounts of sweepback the shapes of the pitching-moment curves were likewise greatly affected by aspect ratio. For example, as shown in figures 15 to 19 for approximately 40° sweepback, the aspect ratio had to be less than 3.5 to insure stability at the stall. With 60° sweepback the aspect ratio had to be less than 1.5 to eliminate instability at the stall as shown in figures 26 to 29.

The results of all the tests of swept-back wings are summarized in figure 41 and show the combined effect of sweepback and aspect ratio on the shape of the pitching-moment curve. The test-point symbols used in figure 41 are the plan forms of the models tested. The solid symbols indicate that the pitching-moment curves indicated instability near the stall and the open symbols indicate that the model did not become unstable but may have shown excessive stability. The cross-hatched symbols indicate pitching-moment curves that showed either a slight increase or decrease in stability at the stall. The cross-hatched boundary in figure 41 may be used as a guide in selecting aspect ratios for wings having different sweepback angles to avoid excessive stability changes for wings alone. The division between stable and unstable wings is unusually clear, with almost no contradictions.

The effect of a decrease in taper ratio λ is generally such as to aggravate tip stalling and thus to increase pitching instability on swept-back wings. For low aspect ratios, however, taper appears to have a beneficial effect on the pitching-moment curves as shown by comparisons of figures 17 and 21 and of figures 19 and 22. This effect requires further study. The final pitching-moment curve for any given wing depends upon such factors as the influence of the tip vortex on the flow over the parts of the wing near the tip and on the location and amount of area in the stalled region as well as on the changes in section pitching-moment characteristics of the stalled regions of the wing.

The effect of a fuselage on the shape of the pitching-moment curve of a wing at the stall cannot be determined conclusively from the data presented but it appears from the location of the wing-fuselage combinations in figure 41 that the fuselage does not have a pronounced effect.

The discussion thus far has dealt only with the pitching-moment curves near maximum lift. Any large change in the pitching-moment curve over any part of the lift range is undesirable even if the change is stabilizing because it would result in undesirable changes in trim and maneuver forces. Some of the swept-back wings had a marked increase in stability at low lift coefficients in addition to the instability at the stall, particularly the wing with 60° sweepback (fig. 26), which showed a marked increase in stability at a lift coefficient of 0.2. The reduction in aspect ratio from 2.55 to 1.0 (fig. 29) required to eliminate completely the instability at the stall also decreased the change in stability at low lift coefficients. For some of the low-aspect-ratio wings having less sweep, the pitching-moment curves showed a continuous increase in stability over the entire lift range. This characteristic was particularly noticeable with the wing of aspect ratio 1.0 having 45° sweepback, as shown in figure 23. It thus appears that if the aspect ratio is too large for a given degree of sweepback, instability at the stall will result; whereas if the aspect ratio is too low, excessive stability at the stall may result.

The results presented thus far have been for wings without the use of any auxiliary stall-control devices. Some success has been had in overcoming instability at the stall by such devices as leading-edge slats, washout, or plan-form modifications. Some results obtained with such devices are shown in figures 39 and 40. In figure 39 a semispan leading-edge tip slat is shown to eliminate the instability of a wing of aspect ratio 7.4 and a sweepback angle of 28°. With the use of 8.5° of twist the instability of a wing with 30° sweepback and aspect ratio 6 was greatly reduced, as shown in figure 40. Appropriate changes in wing section along the span might achieve the same result as geometric washout. Some changes to the wing-tip shape might be beneficial although the results in reference 4 were not very promising. Further research appears to be necessary to insure stability at the stall for tailless airplanes having high-aspect-ratio swept-back wings.

COMPLETE AIRPLANES

The addition of a horizontal tail behind a swept-back wing may be destabilizing, depending upon the rate of change of downwash at the tail location. Figure 45 shows that with a tail added the instability at the stall was eliminated for a wing having an aspect ratio of 5.8 and a sweepback angle of 42°. This horizontal tail was directly behind the wing. That such an improvement is not always realized, however, is shown in figure 44, which indicates that a model which was stable without a horizontal tail became unstable when the tail was added. This tail was behind and somewhat above the wing. Additional tests indicate that the effect of the tail varies greatly with its vertical location and with the aspect ratio of the wing. Downwash effects behind swept-back wings require further investigation before the tail contribution can be predicted accurately.

CONCLUDING REMARKS

From a study of available data on swept-back wings at low speeds it appears possible to maintain longitudinal stability at the stall by selecting the proper aspect ratio. The addition of a horizontal tail behind swept-back wings may be destabilizing and requires further investigation.

Langley Memorial Aeronautical Laboratory
National Advisory Committee for Aeronautics
Langley Field, Va., May 2, 1946

REFERENCES

1. Anderson, Raymond F.: Determination of the Characteristics of Tapered Wings. NACA Rep. No. 572, 1936.

2. Letko, William, and Goodman, Alex: Preliminary Wind-Tunnel Investigation at Low Speed of Stability and Control Characteristics of Swept-Back Wings. NACA TN No. 1046, 1946.

3. Weick, Fred E., and Sanders, Robert: Aerodynamic Tests of a Low Aspect Ratio Tapered Wing with Various Flaps, for Use on Tailless Airplanes. NACA TN No. 463, 1933.

4. Seacord, Charles L., Jr., and Ankenbruck, Herman O.: Effect of Wing Modifications on the Longitudinal Stability of a Tailless All-Wing Airplane Model. NACA ACR No. L5G23, 1945.

5. Göthert, B.: Hochgeschwindigkeitsmessungen an einem Pfeilflügel (Pfeilwinkel $\varphi = 35^\circ$). Bericht 156 der Lilienthal-Gesellschaft für Luftfahrtforschung, 1942, pp. 30-40.

6. Anon.: Air Force and Moment for Gliding Wing. Rep. No. 677, Aerod. Lab., Dept. Aero., Washington Navy Yard, Aug. 21, 1943.

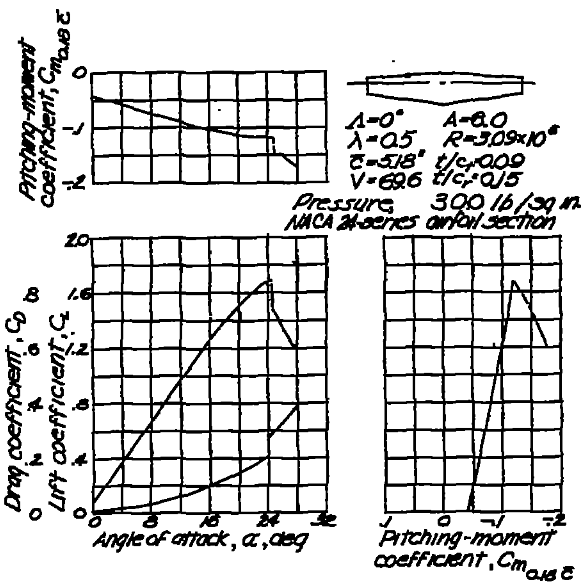

Figure 1.- Longitudinal stability characteristics of a 0° swept-back wing. Data from reference 1.

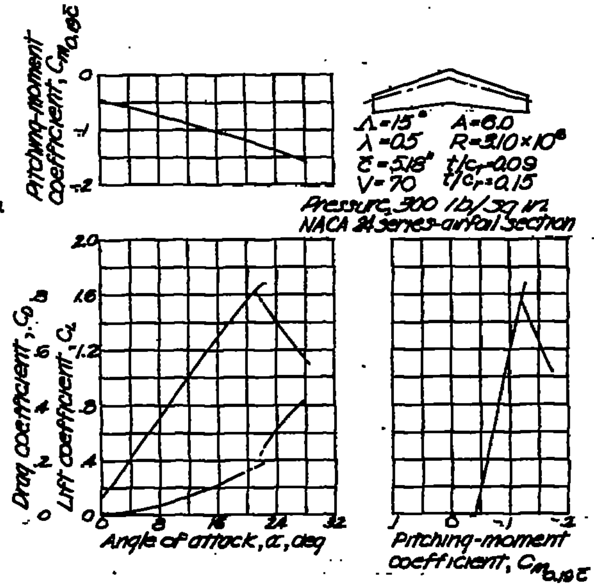

Figure 2.- Longitudinal stability characteristics of a 15° swept-back wing. Data from reference 1.

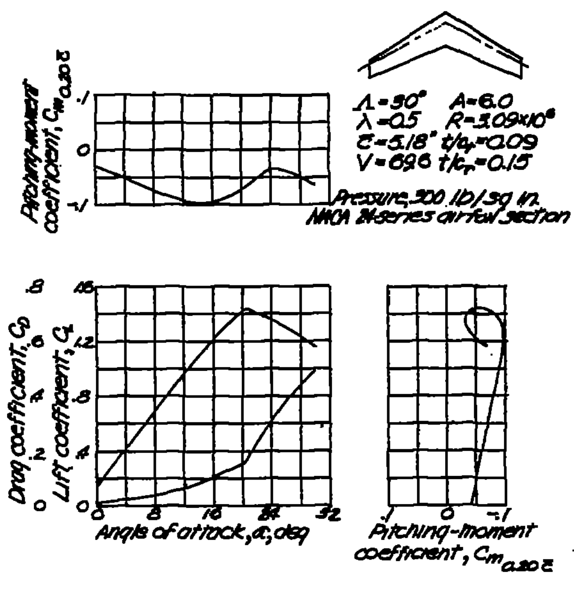

Figure 3.- Longitudinal stability characteristics of a 30° swept-back wing. Data from reference 1.

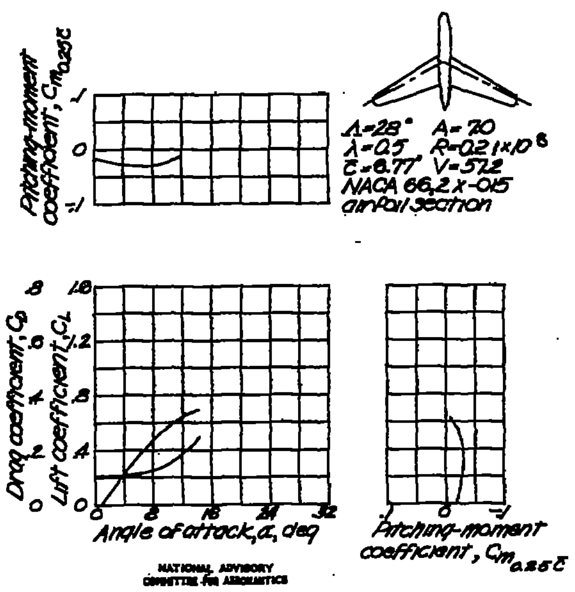

Figure 4.- Longitudinal stability characteristics of a 28° swept-back wing and fuselage combination. Data from the Langley free-flight tunnel.

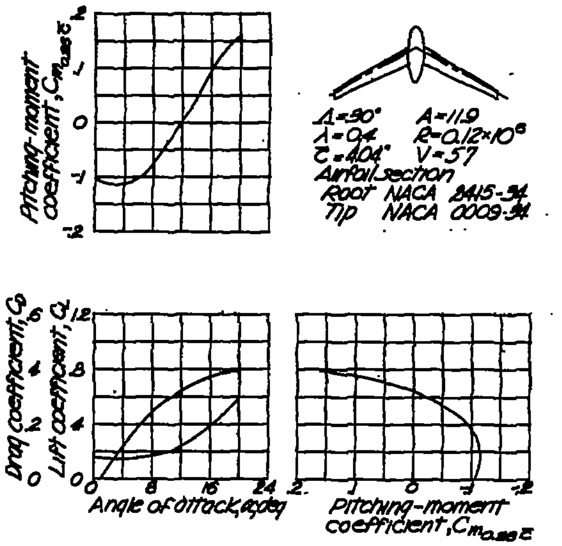

Figure 5.- Longitudinal stability characteristics of a 30° swept-back wing and fuselage combination. Data from Langley free-flight tunnel.

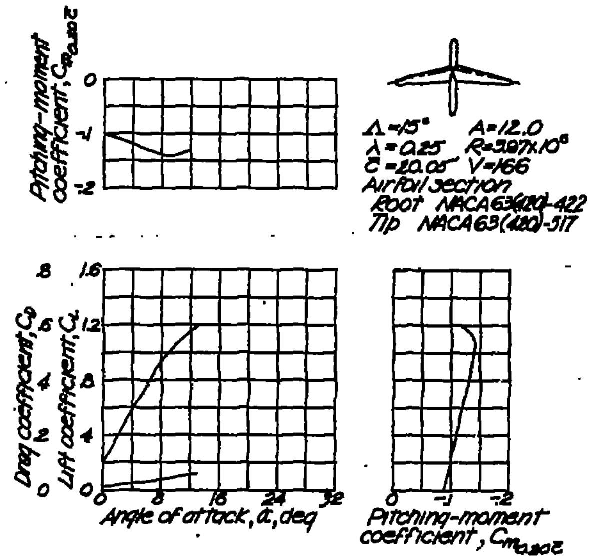

Figure 6.- Longitudinal stability characteristics of a 15° swept-back wing and fuselage combination. Data from Langley 19-foot pressure tunnel.

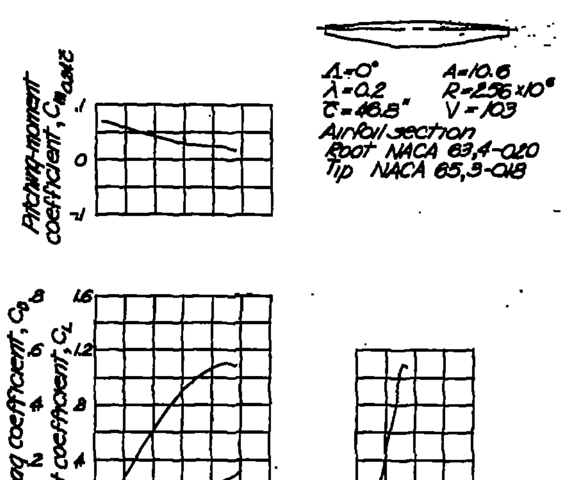

Figure 7.- Longitudinal stability characteristics of a 0° swept-back wing. Data from the Langley full-scale tunnel.

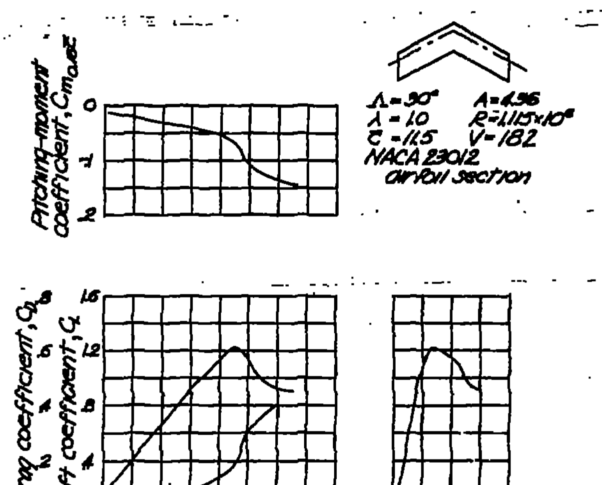

Figure 8.- Longitudinal stability characteristics of a 30° swept-back wing. Data from reference 2.

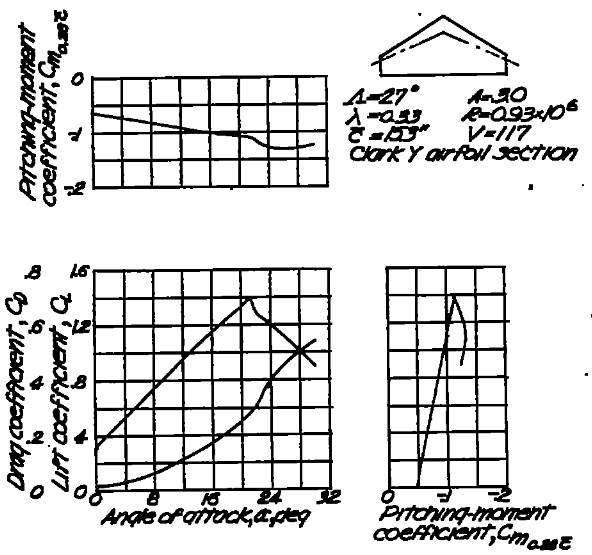

Figure 9.- Longitudinal stability characteristics of a 27° sweptback wing. Data from reference 3.

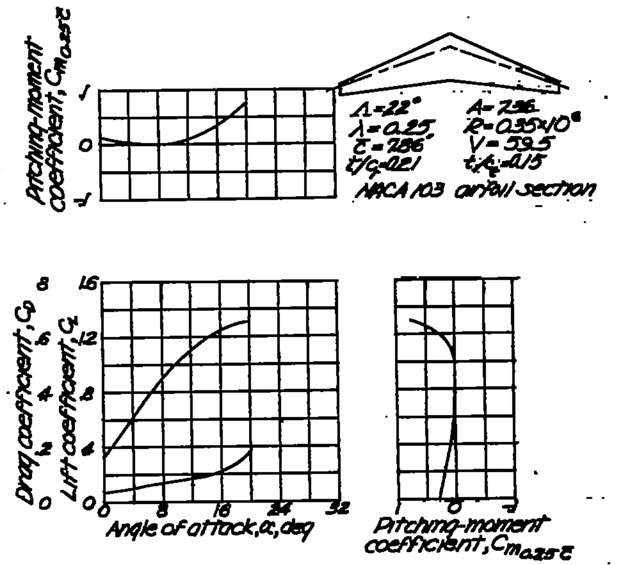

Figure 10.- Longitudinal stability characteristics of a 22° swept-back wing. Data from reference 4.

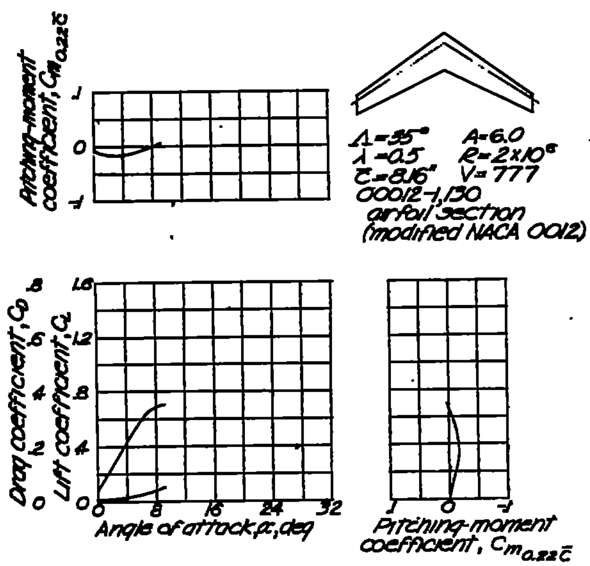

Figure 11.- Longitudinal stability characteristics of a 35° swept-back wing. Data from reference 5.

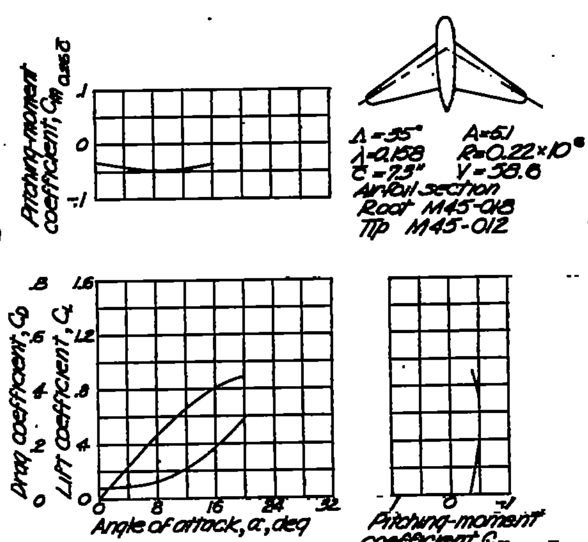

NATIONAL ADVISORY COMMITTEE FOR AERONAUTICS

Figure 12.- Longitudinal stability characteristics of a 35° swept-back wing and fuselage combination. Data from Langley free-flight tunnel.

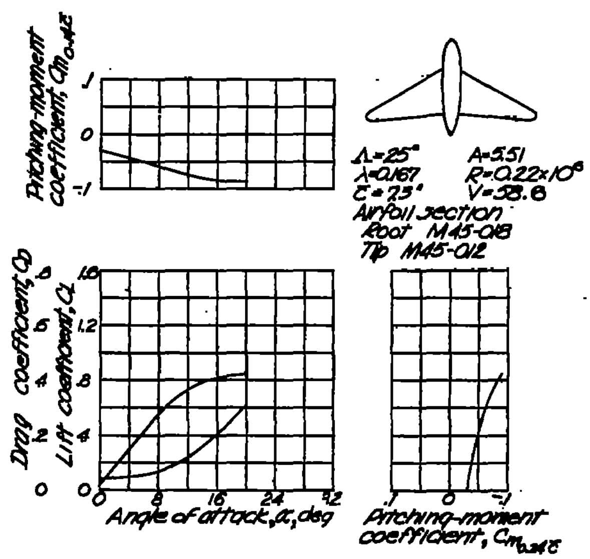

Figure 13.- Longitudinal stability characteristics of a 25° swept-back wing and fuselage combination. Data from the Langley free-flight tunnel.

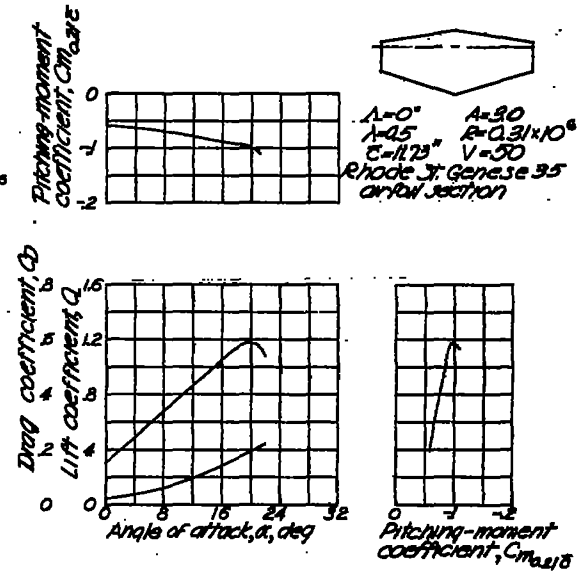

Figure 14.- Longitudinal stability characteristics of a 0° swept-back wing. Data from the Langley free-flight tunnel.

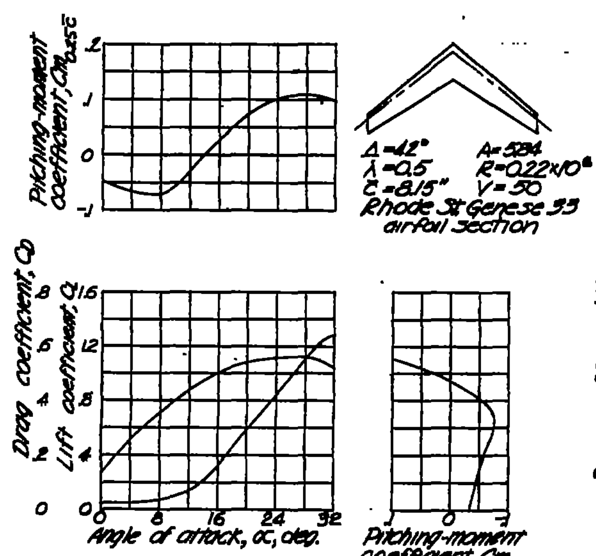

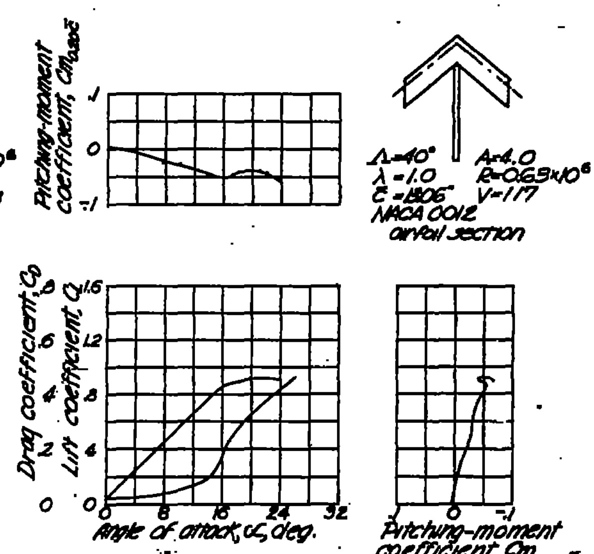

NATIONAL ADVISORY COMMITTEE FOR AERONAUTICS

Figure 15.- Longitudinal stability characteristics of a 42° swept-back wing. Data from the Langley free-flight tunnel.

Figure 16.- Longitudinal stability characteristics of a 40° swept-back wing. Data from the Langley 7-by 10-foot tunnel.

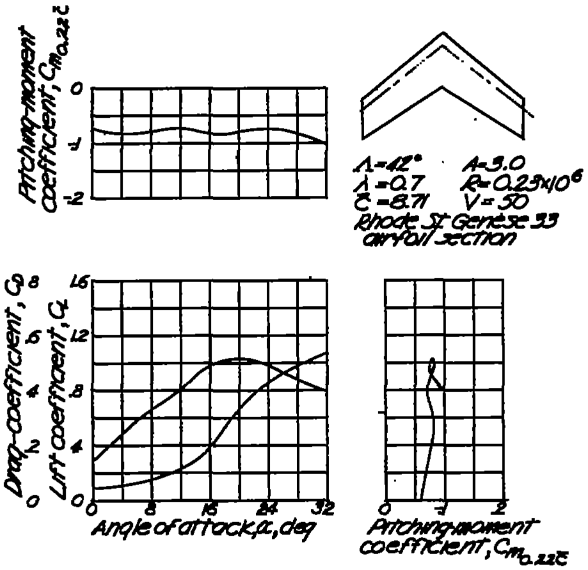

Figure 17.- Longitudinal stability characteristics of a 42° swept-back wing. Data from the Langley free-flight tunnel.

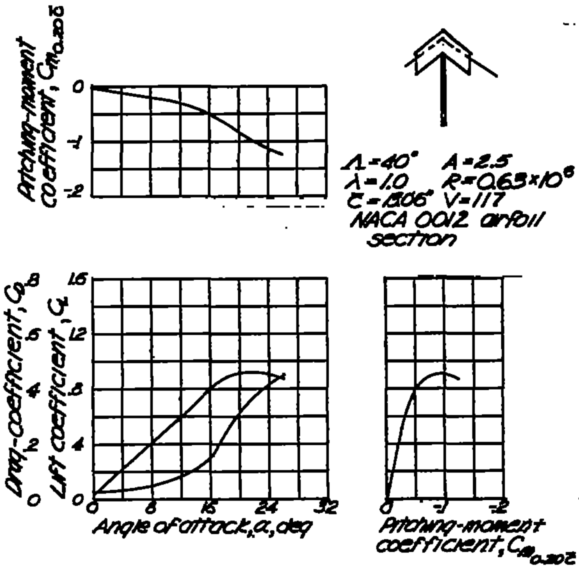

Figure 18.- Longitudinal stability characteristics of a 40° swept-back wing. Data from the Langley 7-by 10-foot tunnel.

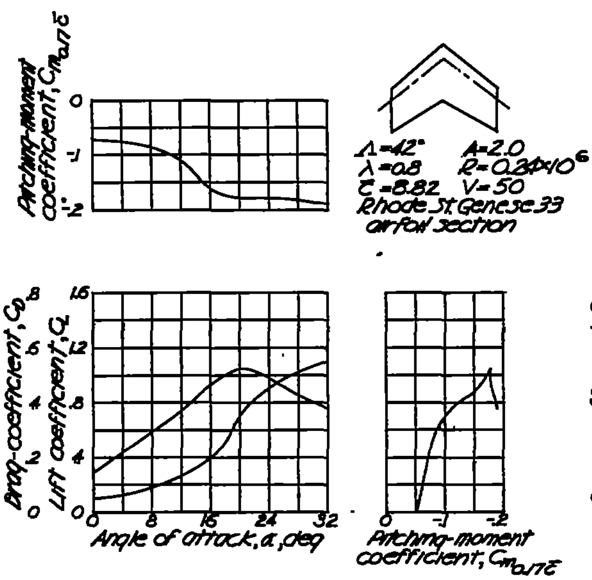

Figure 19.- Longitudinal stability characteristics of a 42° swept-back wing. Data from the Langley free-flight tunnel.

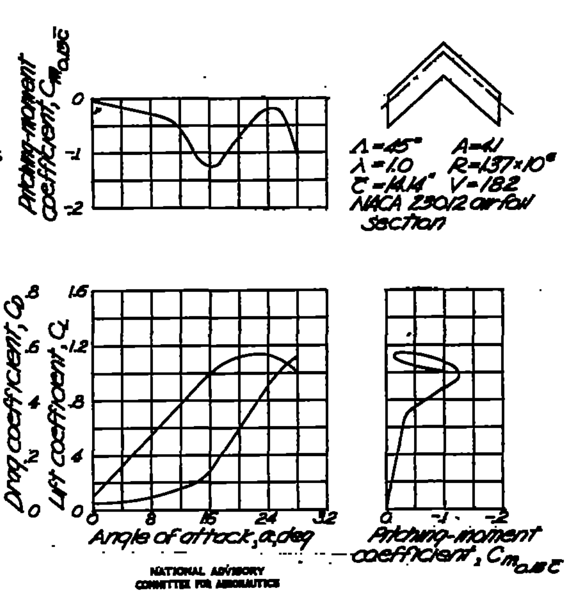

Figure 20.- Longitudinal stability characteristics of a 45° swept-back wing. Data from reference 2.

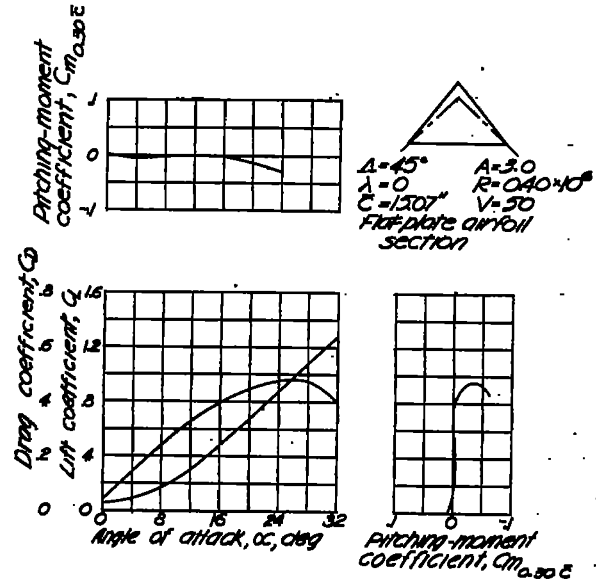

Figure 21.- Longitudinal stability characteristics of a 50° swept-back wing. Data from the Langley free-flight tunnel.

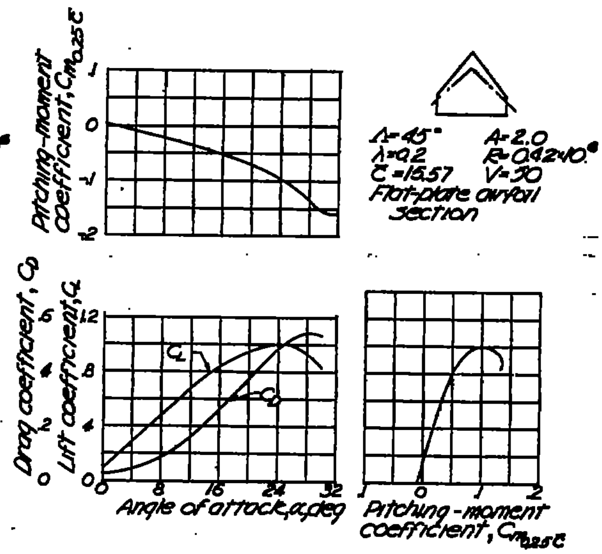

Figure 22.- Longitudinal stability characteristics of a 50° swept-back wing. Data from the Langley free-flight tunnel.

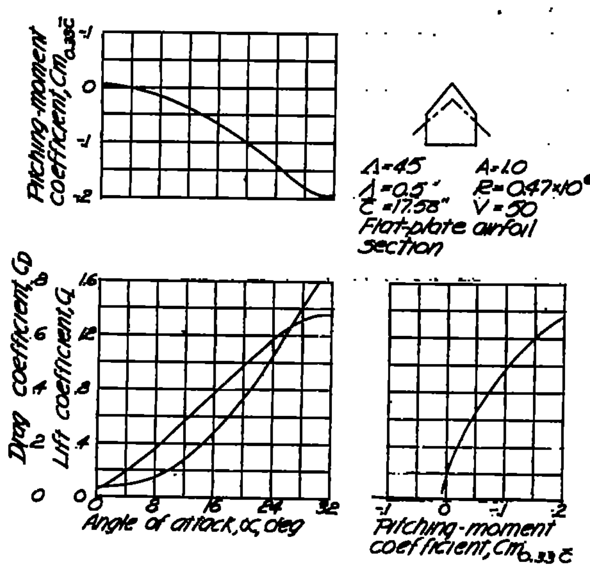

Figure 23.- Longitudinal stability characteristics of a 50° swept-back wing. Data from the Langley free-flight tunnel.

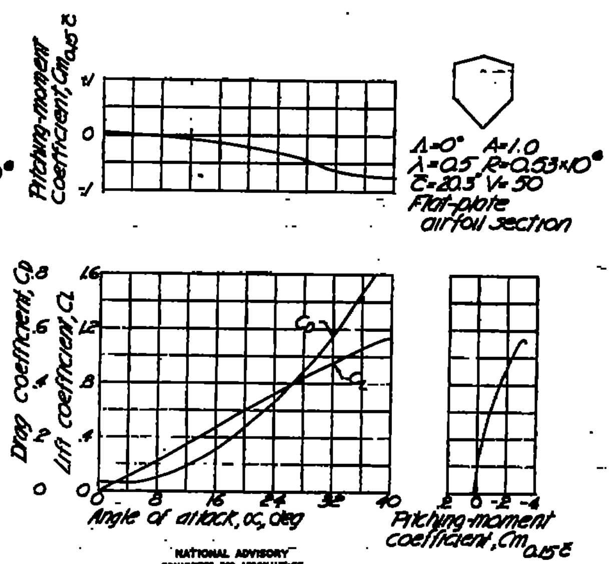

Figure 24.- Longitudinal stability characteristics of a 0° swept-back wing. Data from the Langley free-flight tunnel.

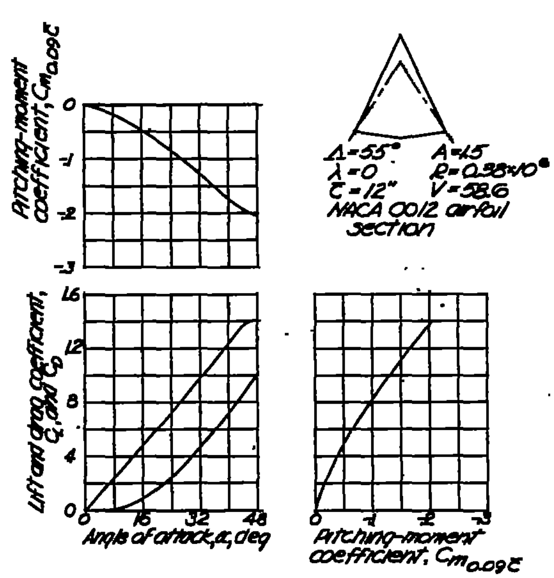

Figure 25.- Longitudinal stability characteristics of a 55° swept-back wing. Data from reference 6.

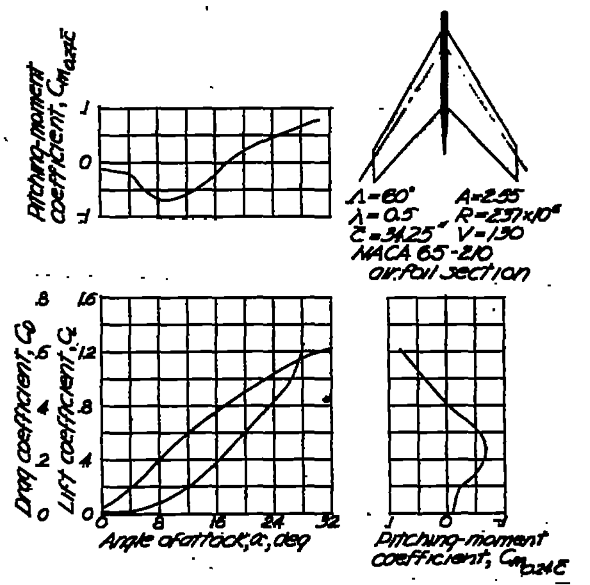

Figure 26.- Longitudinal stability characteristics of a 60° swept-back wing. Data from the Langley 300 MPH 7-by 10-foot tunnel.

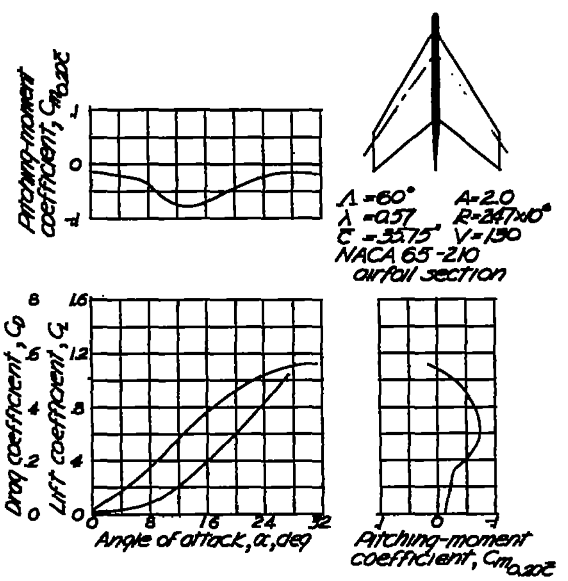

Figure 27.- Longitudinal stability characteristics of a 60° sweptback wing. Data from the Langley 300 MPH 7-by 10-foot tunnel.

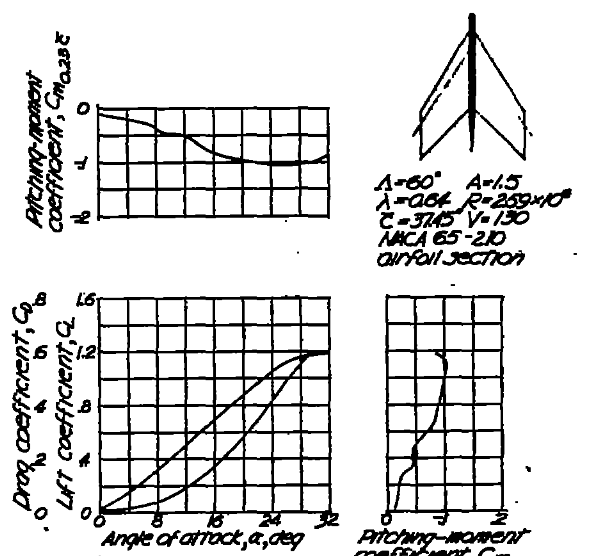

NATIONAL ADVISORY COMMITTEE FOR AERONAUTICS

Figure 28.- Longitudinal stability characteristics of a 60° swept-back wing. Data from the Langley 300 MPH 7-by 10-foot tunnel.

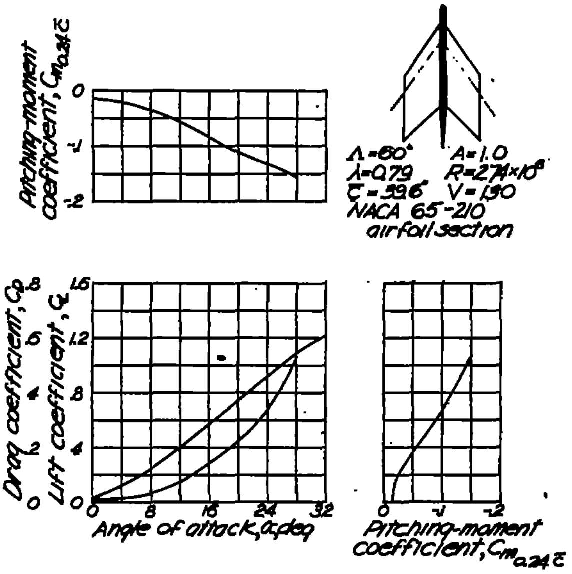

Figure 29.- Longitudinal stability characteristics of a 60° swept-back wing. Data from the Langley 300 MPH 7-by 10-foot tunnel.

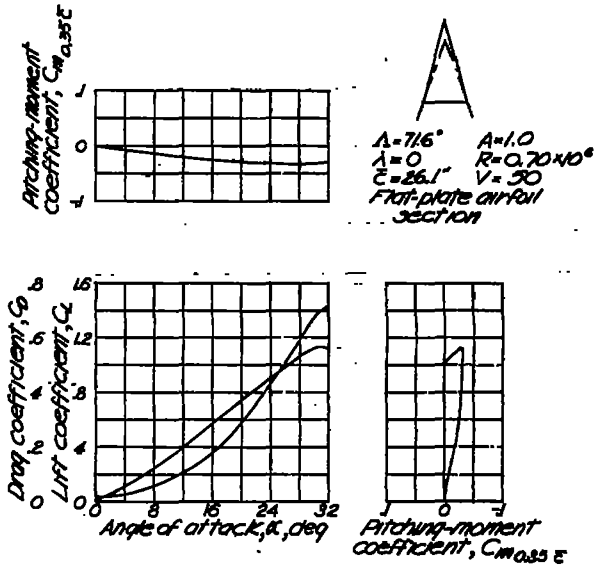

Figure 30.- Longitudinal stability characteristics of a 71.6° swept-back wing. Data from the Langley free-flight tunnel.

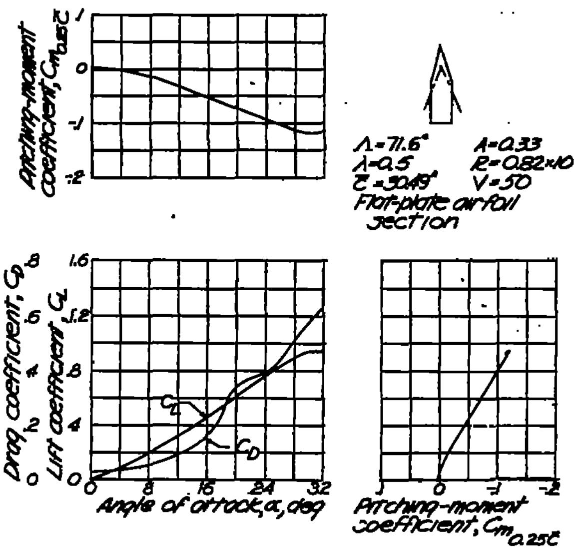

Figure 31.- Longitudinal stability characteristics of a 71.6° swept-back wing. Data from the Langley free-flight tunnel.

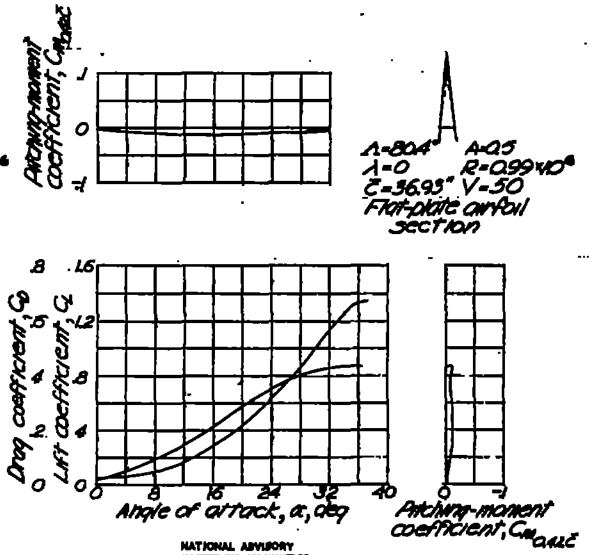

NATIONAL ADVISORY COMMITTEE FOR AERONAUTICS

Figure 32.- Longitudinal stability characteristics of an 80.4° swept-back wing. Data from the Langley free-flight tunnel.

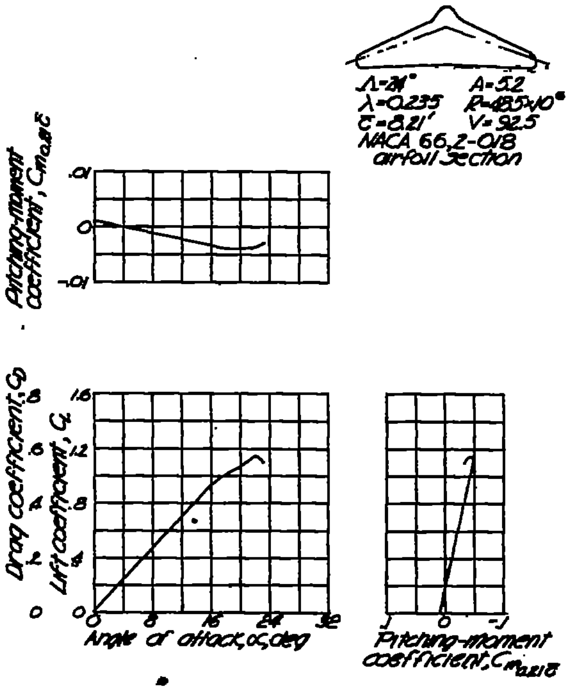

Figure 33.- Longitudinal stability characteristics of a 24° swept-back wing. Data from the Langley full-scale tunnel.

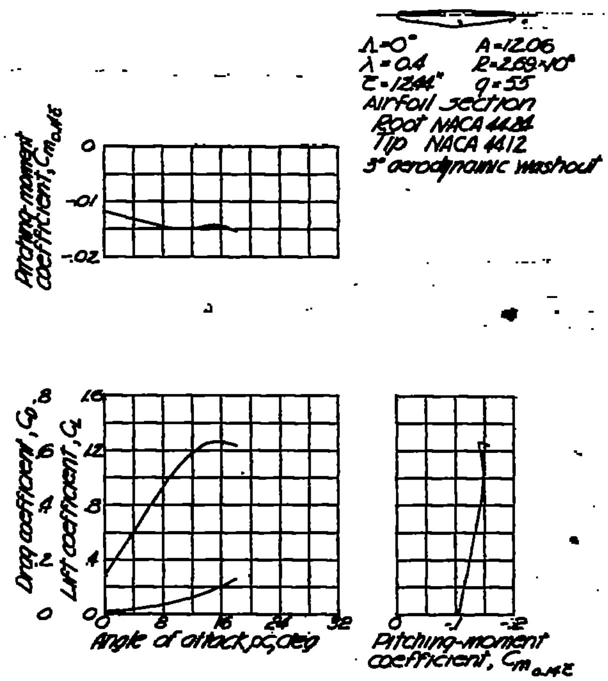

Figure 34.- Longitudinal stability characteristics of a 0° swept-back wing. Data from Langley 19-foot pressure tunnel.

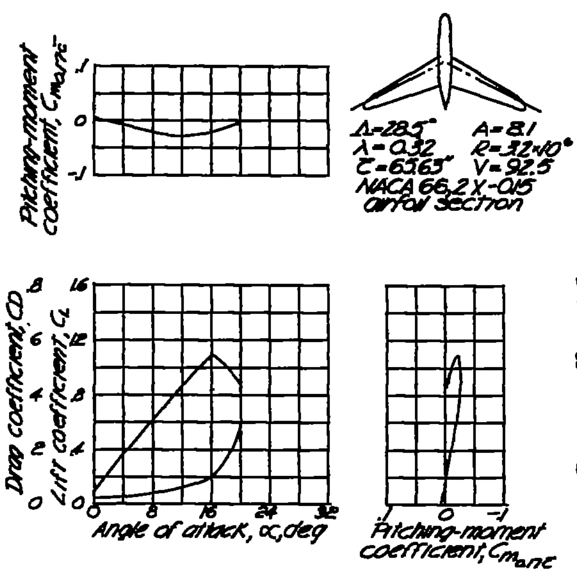

Figure 35.- Longitudinal stability characteristics of a 28.5° swept-back wing and fuselage combination. Data from the Langley full-scale tunnel.

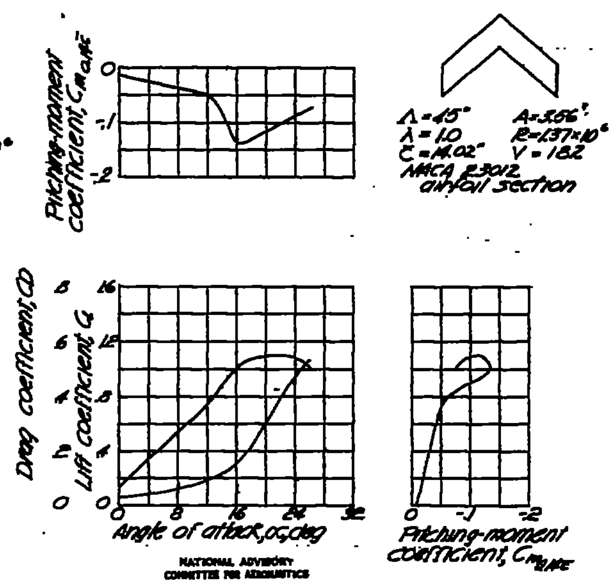

Figure 36.- Longitudinal stability characteristics of a 45° swept-back wing. Data from reference 2.

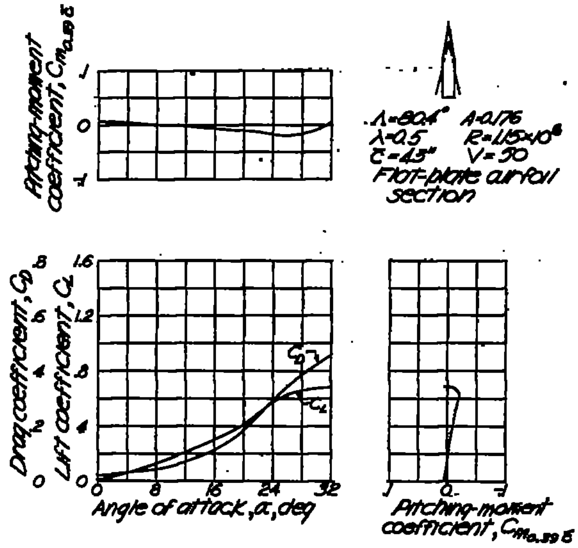

Figure 37.- Longitudinal stability characteristics of a 80.4° swept-back wing. Data from the Langley free-flight tunnel.

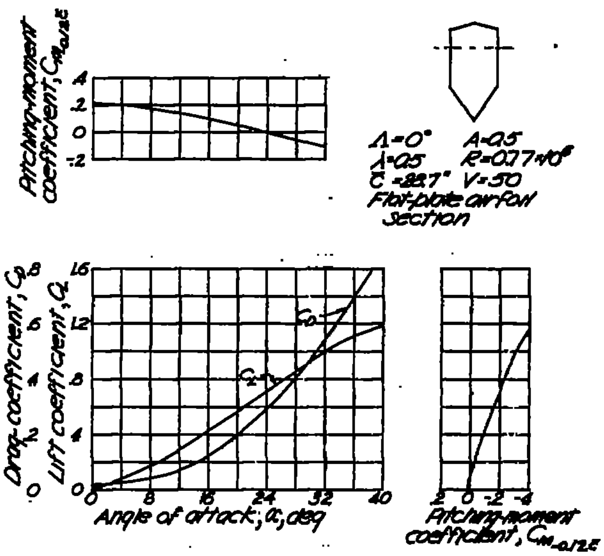

Figure 38.- Longitudinal stability characteristics of a 0° swept-back wing. Data from the Langley free-flight tunnel.

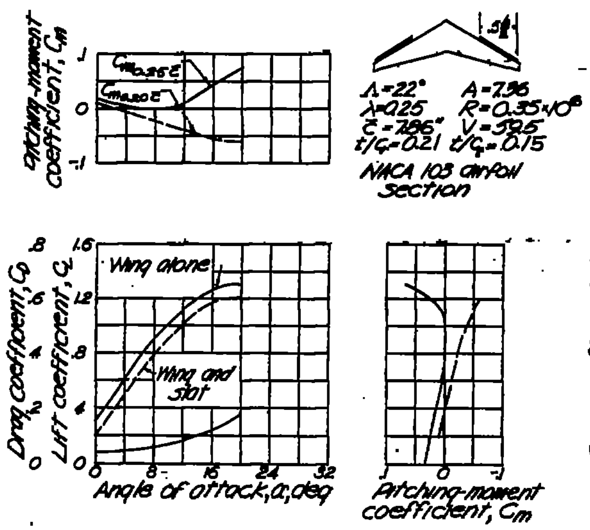

Figure 39.- Effect of slats on the longitudinal stability characteristics of a 22° swept-back wing. Data from reference 4.

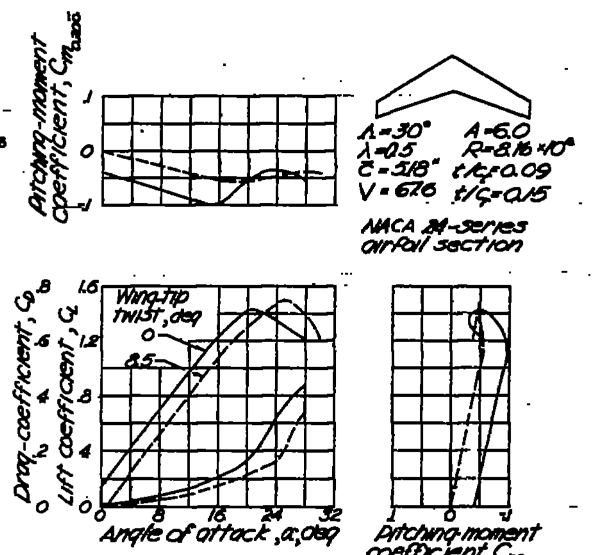

NATIONAL ADVISORY COMMITTEE FOR AERONAUTICS

Figure 40.- Effect of wing-tip twist on the longitudinal stability characteristics of a 30° swept-back wing. Data from reference 1.

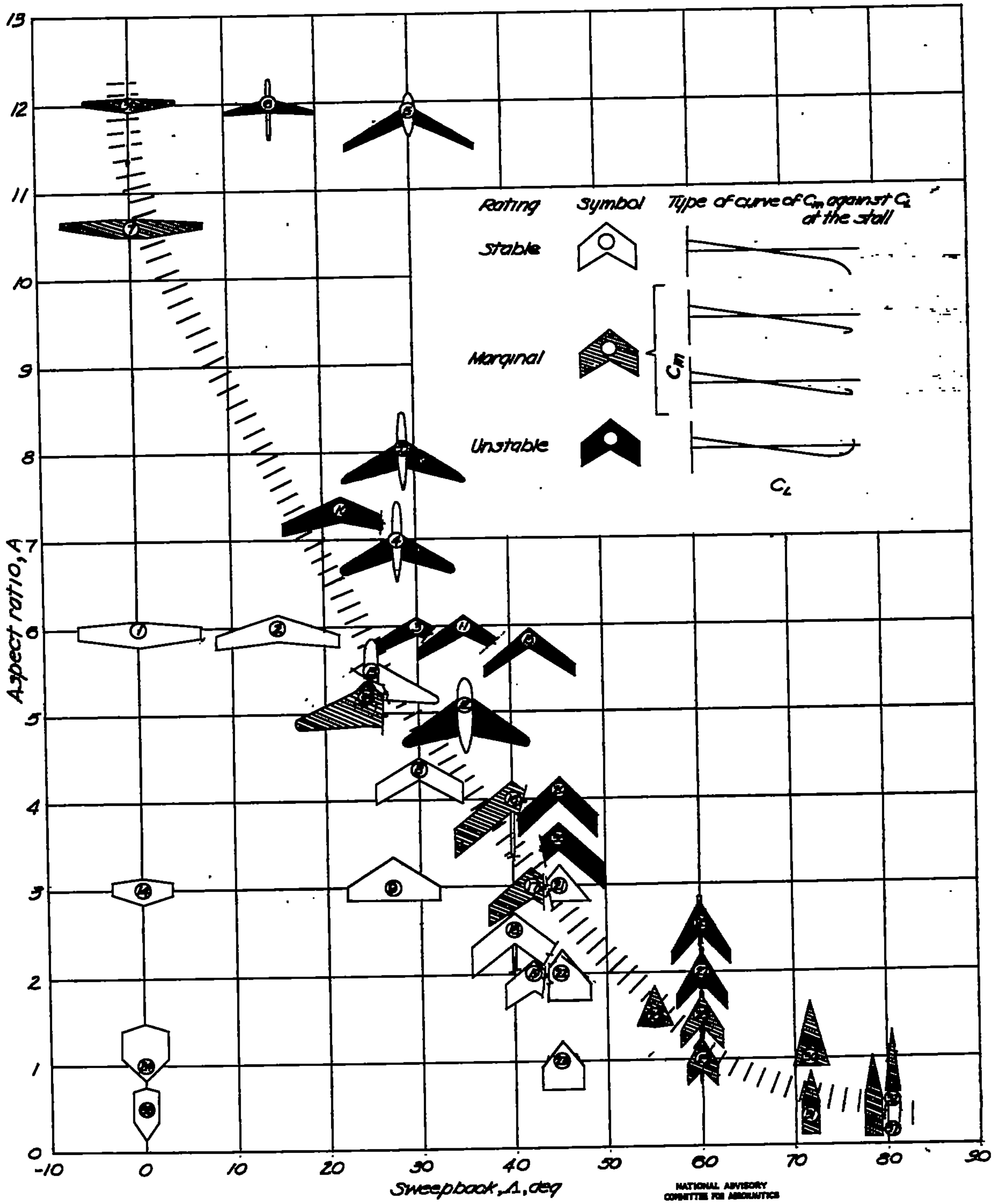

Figure 41.- Chart summarizing the effect of aspect ratio on the pitching-moment curve of swept-back wings at the stall. Position of circle defines aspect ratio and sweepback and number in circle indicates figure in which longitudinal stability characteristics are presented.

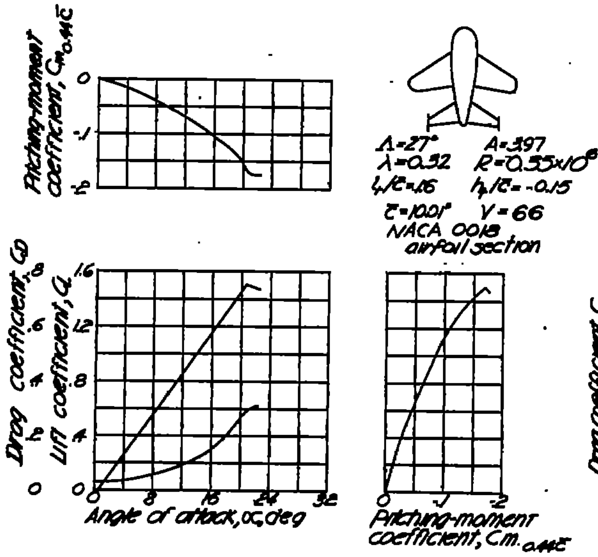

Figure 42.-Longitudinal stability characteristics of a complete airplane model with a 27° swept-back wing. Data from GALCIT.

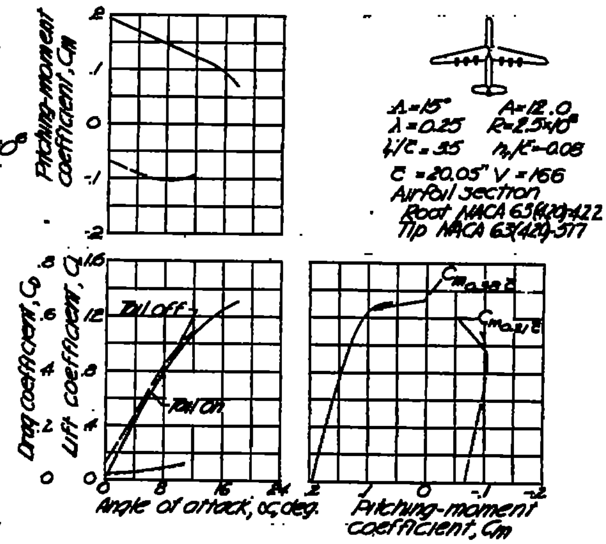

Figure 43.-Longitudinal stability characteristics of a complete airplane model with a 15° swept-back wing. Data from the Langley 19-foot pressure tunnel.

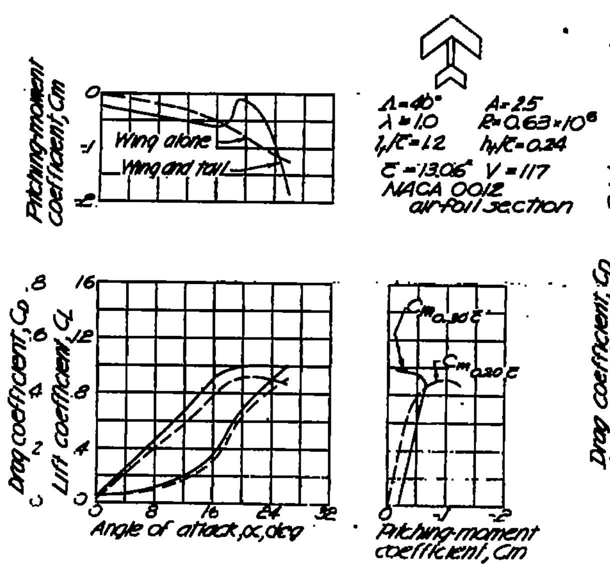

Figure 44.-Longitudinal stability characteristics of a 40° swept-back wing and horizontal tail combination. Data from the Langley 7 by 10 foot tunnel.

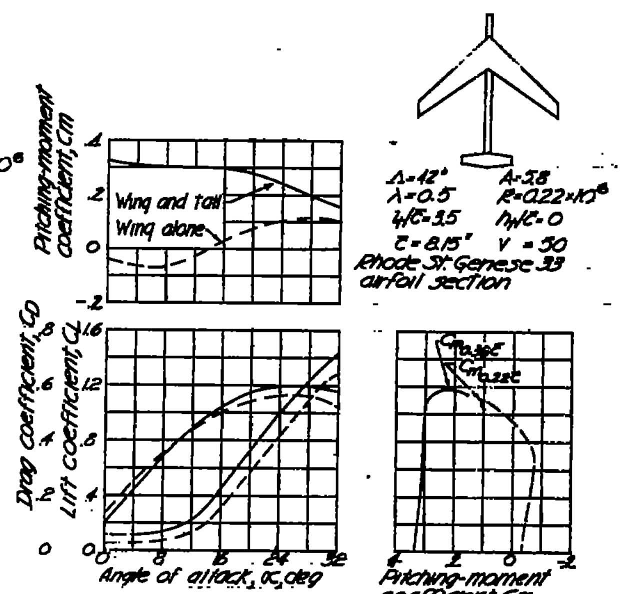

NATIONAL ADVISORY COMMITTEE FOR AERONAUTICS

Figure 45.-Longitudinal stability characteristics of a 42° swept-back wing and horizontal tail combination. Data from the Langley free-flight tunnel.